Charge transport properties of Nd_2O_3 embedded ZnO nanowires/nanoplates

Naresh and Rakesh Dhar
Department of Physics, Guru Jambheshwar University of Science &Technology, Hisar,India-125001
Corresponding author: Prof. Rakesh Dhar E-mail:rakesh285@gmail.com

Abstract

ZnO/Nd_2O_3 nanowires/plates were synthesized on glass substrate using the thermal evaporation technique in five different loading concentrations i.e. 1, 2, 3, 5, 7 wt% of Nd_2O_3 in ZnO matrix. The structural, molecular bonding, morphological properties of prepared nanocomposite samples were investigated using the X-ray diffraction (XRD), Fourier transform infrared (FTIR) spectroscopy, and Field emission scanning electron microscope (FESEM), respectively. XRD patterns of prepared samples reveal that prepared samples have semi-crystalline structure, whereas, FTIR spectra contain all required fundamental bands which confirms the growth of desired samples. FESEM indicates that prepared samples have nanowires/plates like morphology. The electrical properties of these samples were also investigated using the I-V characteristics, and charge transport mechanism was investigated using Arrhenius's and modified Kivelson's model. The electrical conductivity of prepared nanowires composite samples increases with the increase in doping concentration as well as increase in temperature which indicates the semiconducting behaviour of these nanocomposites. The, prepared are further utilized for ethanol vapors detection measurements. The 7% Nd2O3 deoped ZnO sample contains maximum sensing response % i.e. ~30% at 200 ppm level and 200 °C.

Keywords: Thermal; Evaporation; Conduction; Arrhenius; ethanol.
DOI Number: 10.14704/nq.2022.20.5.NQ22722 NeuroQuantology 2022; 20 (5):4382-4393

Introduction

ZnO is an n-type and most commonly used semiconductor which has lot of tremendous applications in such as sensor, laser, solar cell, antimicrobial, electronic and chemical devises, etc. due to its significant chemical and physical properties [1-3]. However, the properties of ZnO can be influenced by the growth of composite samples, hetero-junction, doping, and various synthesis routes [4-7]. ZnO semiconductor can be synthesized using various procedures like as solochemical, hydrothermal, and precipitation [8-10]. Out of these synthesis routes, the precipitation process is simple, widely and low cost synthesis technique at large scale production in industries [11]. Besides this, the solochemical procedure is completely based upon the chemical reactions produced by adding metallic precursor to the heated alkaline solution at controlled temperature and slow reagent combination. This synthesis method is also considered as fast, simple and inexpensive but there is no need to additive and heat treatment at very high temperatures for oxide production, by product formation, avoiding parallel reactions, and additional costs with complex equipment [12].

However, the nanocomposites can be prepared of ZnO with different types of metals, oxides, non-metals, lanthanides, which can enhance the antimicrobial, photocatalytic, optical properties, theseproperties can createnew active sites and can cause reduction in electron-hole pair recombination rate [13-15]. The rare earth metal Neodymium pristine and its oxides can also be used as doping materials in ZnO matrix to enhance the physical and chemical properties [16,17]. Therefore, in the present study, we have been synthesized ZnO/Nd_2O_3 nanocomposites (with different doping concentrations 1, 2, 3, 5 and 7 wt% of Nd_2O_3 nanoparticles in ZnO matrix), and their structural, molecular bonding and morphological properties have been investigated. Thereafter, the electrical properties of presently prepared composite samples were also investigated because the doping and its level of Nd_2O_3 nanoparticles directly affect the electrical properties of ZnO, and this enhancement in electrical properties is evident to utilization of these composites in various applications. Thus the ethanol vapors detection properties of prepared samples were investigated in different ethanol vapors.

Experimental Details

Synthesis of ZnO/Nd_2O_3 nanocomposites

The chemicals required for synthesis of ZnO/Nd_2O_3 nanocomposites were purchased from sigma Aldrich (purity >99.99%). For the present study, we have been prepared five different Nd_2O_3 (1, 2, 3, 5 and 7 wt%) doped ZnO based composite samples in the form of thin film deposited on glass slides. In the typical deposition process, thermal evaporation technique was used at high vacuum pressure $8x10^{-6}$ mbar with the help of combination of diffusion and rotary pump. In this system, we are used two different molybdenum boats to evaporate the ZnO (99 wt%) and Nd_2O_3 (1 wt%). These two boats connected with two different low tension supplies for enabling the dual-evaporation of both the materials. As we know, different materials have different melting/sublimation points, thus we could supply the optimum values of current to both the boats containing ZnO (melting point ~ 1975 ^oC) and Nd_2O_3 (melting point ~120 ^oC) for the simultaneous evaporation of both compounds. However, glass substrate was used for the deposition of thin films. Before considering as substrate, the glass slides were priory cleaned using the soap and chemical cleaning. After that glass substrates were dried using the nitrogen gas blowing, then cleaned glass substrate were mounted at the substrate holder at equidistant (18 cm) from the both boats at the vertical distance. Thereafter the values of applied current was gradually increased by rotating the knob of current controller unit to low tension power supply till both the boats become red hot as well as evaporation of materials was initiated. The entire process was monitored through the transparent glass window, and the deposited thin films were annealed at 450° C temperature for 2 hrs in vacuum chamber itself using substrate heater in rough vacuum of 10^{-3} mbar. Next day, after cooling the samples, deposited thin films removed out and cut in desired surface area for further characterization. The similar synthesis route was followed for four other different doping concentrations of Nd_2O_3 i.e. 2, 3, 5 and 7 wt% in ZnO matrix, and named as S2, S3, S4, and S5, respectively.

Characterization Techniques

Thermal evaporation technique (Vacuum Technique Pvt. Ltd. Bengaluru, India,) was employed for the deposition process.The structural analysis of the prepared samples was carried out using X-ray diffractometer (XRD; Rigaku made) with CuKα, λ=1.54174Å radiation. The molecular spectra of ZnO/Nd_2O_3composite samples were recorded using Fourier transform infrared (FTIR) spectrometer (make Perkin Elmer, model 783). The morphological investigation of prepared samples was done using high resolution field emission scanning electron microscopy (FESEM Model-7610F Plus/JEOL). The temperature dependent dc conductivity measurements were carried out on

Keithley's 6517B electro-measure unit (EMU) in the temperature range of 303-393K.

Result and Discussions

X-Ray Diffraction and Vibrational Spectroscopic Measurements

The structural and crystallinity properties of prepared ZnO/Nd_2O_3nanocomposite thin film samples were investigated using XRD as shown in figure 1a. From the figure, it is observed that the prepared samples have almost amorphous matrix as shown in XRD patterns of 1 and 2 wt% Nd_2O_3 doped ZnO samples S1 and S2, whereas, the 3, 5 and 7 wt% Nd_2O_3 doped ZnO samples S2, S3 and S4 contains some highly intense peaks at angle 2θ ≈31.46, 35.94, 38.64 and 42.92°, these peaks are associated with the hkl planes 100, 101, 102 and 110, respectively. The presence of these peaks indicates that ZnO/Nd_2O_3 composite samples are in hexagonal phase [18], according to JCPDS file no. (36-1451) [19]. Moreover, it can also be observed as the doping of Nd_2O_3 particles in ZnO matrix increases, the intensity of these peaks also increases which is showing the increase in crystalline character of ZnO composite samples.

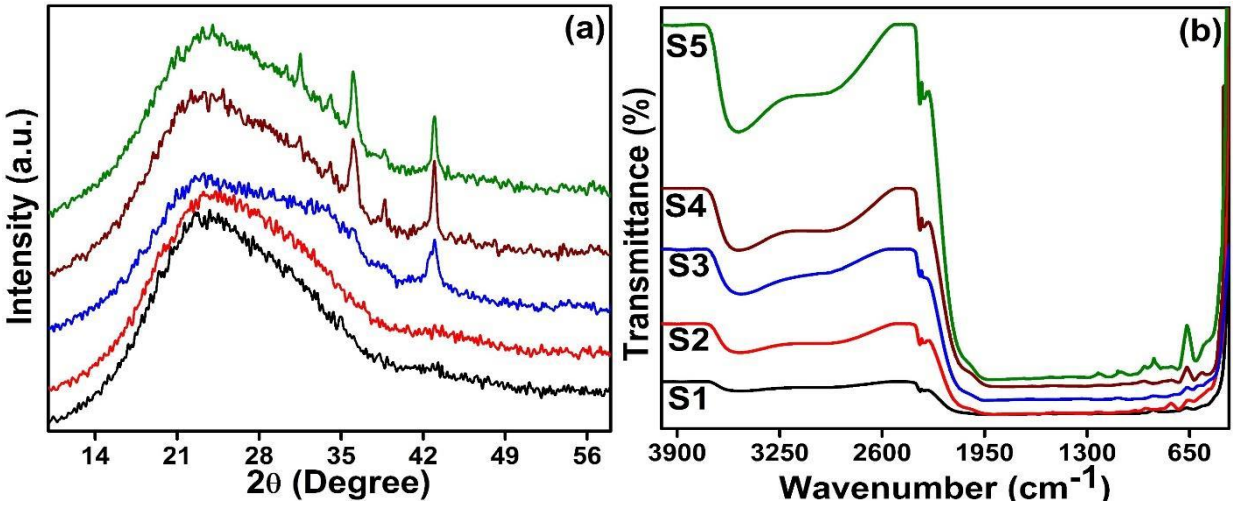

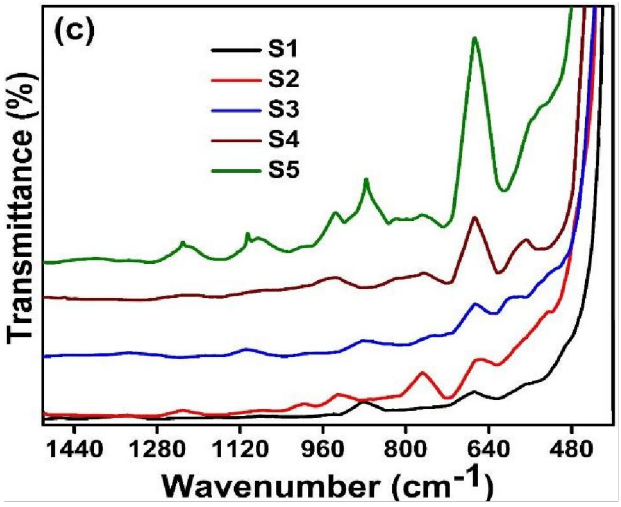

Figure 1: (a) XRD pattern, FTIR spectra in the wavenumber range (b) 4000 to 400 cm^{-1}, and (c) 1500-400 cm^{-1} for the S1-S5 samples.

The molecular bonding measurements for the identifications of functional groups were carried out using the FTIR in the wave number range 4000-400 cm^{-1}. Figure 1b elucidates the FTIR spectra of prepared samples S1, S2, S3, S4 and S4 along with the required fundamental bands. The band situated at around ~3514 cm^{-1} is associated with the O-H stretching due to Nd_2O_3, whereas, the one situated at around ~2986 cm^{-1} is attributed with the NH_2 stretching vibration. Moreover, to investigate the exact variation in peaks with the increase in doping concentration, the FTIR spectrum plotted in the wavenumber range 1500-400 cm^{-1}, as shown in figure 1c. Here, the band situated at around ~532 cm^{-1} is associated with the Zn-O molecular bonding, whereas, band observed at around ~618 cm^{-1} is attributed with Nd-O molecular bonding. The band situated at around ~1294 cm^{-1} is associated with the $–CH_2–$ bonding state. Also, a doublet is observed at around ~720 and 836 cm^{-1} which belongs to bonding states Nd-O-Zn. The triplet situated at around ~922, 1030 and 1152 cm^{-1} is attributed with the oxide stretching of Nd and Zn, respectively [20,21].

The morphological properties of prepared composite samples S2 and S3 were investigated using the FESEM (figure 2a,b). From the figures, it is observed that prepared samples have nanowires/plates like morphology and these nanowires/plates have thickness 15-20 nm, whereas, length is ~100 nm.Furthermore, to investigate the elemental concentrations in prepared samples, the EDX studies have been carried out on both the composite samples and observed elements were tabulated in table 1.

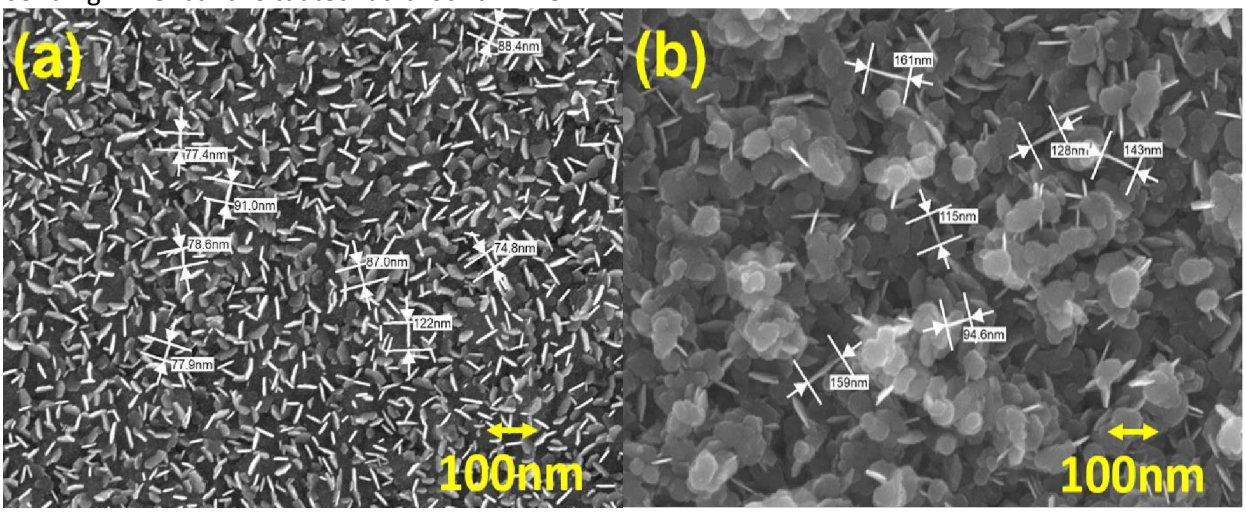

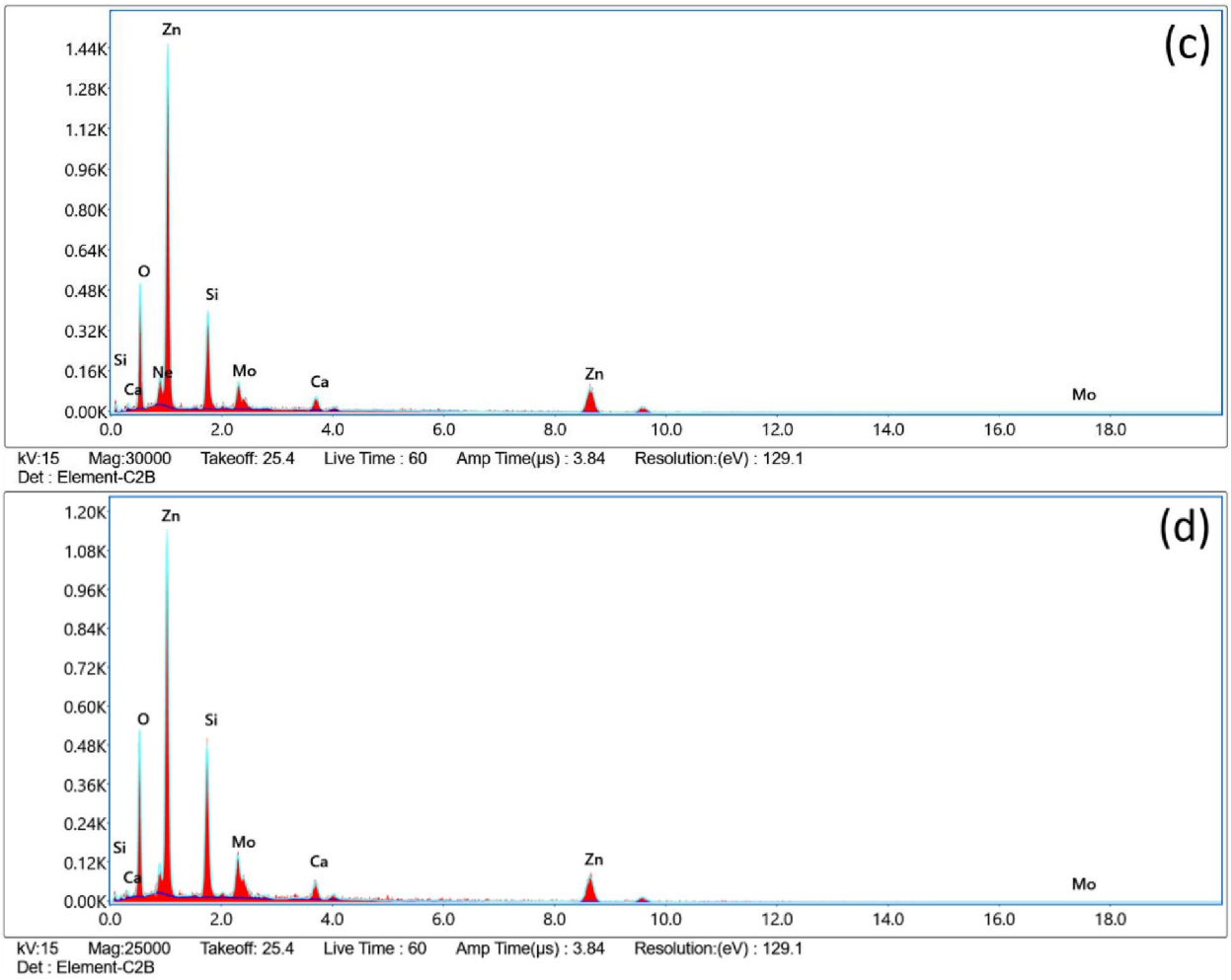

Figure 2:FESEM images of (a) S2 and (b) S3 samples, and EDX data of (c) S2 and (d) S3 sample.

Table 1 Elemental concentration (%) in ZnO/Nd_2O_3 composite samples S2 and S3

Elements	**Elemental Concentration (%) in Samples**	
	S2	**S3**
O	19.51	25.76
Ne	0.62	------
Zn	58.73	45.08
Si	11.30	15.25
Mo	6.91	10.25
Ca	2.93	3.65

Electrical conductivity Measurements

To investigate the effect of Nd_2O_3 nanoparticles in ZnO matrix, current-voltage (I-V) measurements carried out through Keithley's electrometer 6517B in the temperature range 303-393 Kand voltage range -10 to +10 V, for all the prepared samples S1, S2, S3, S4 and S5 as shown in figure 3.

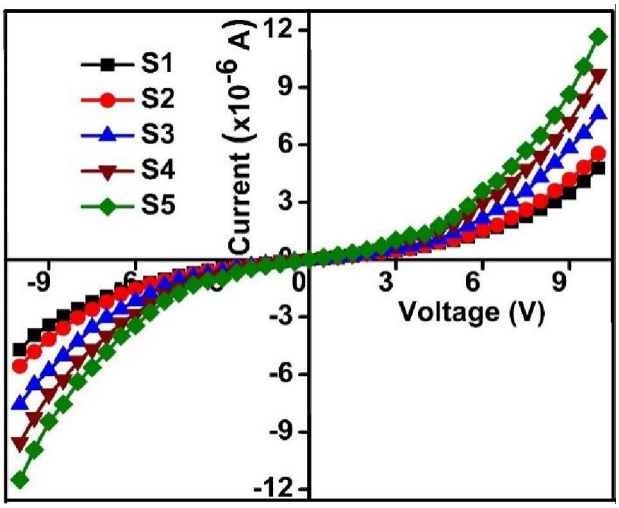

Figure 3: Current-Voltage (I-V) characteristics of Nd_2O_3 doped ZnO based samples (S1-S5).

From the figure it is observed that the values of current increases with the increase in applied voltage. The increase in current with voltage is not linear, and that is ohmic-like increase which indicates prepared samples follow semiconductor behavior for charge transport mechanism.

The high temperature (393K) electrical conductivity values estimated to be $0.41x10^{-3}$, $0.47x10^{-3}$, $0.54x10^{-3}$, $0.62x10^{-3}$ and $0.69x10^{-3}$, for the samples S1, S2, S3, S4 and S5, respectively. The electrical conductivity of prepared samples increases with the increase in doping concentration. In the composite materials, the charge transport behaviour is generally governed by semi-classical (Drude) model, but the situation is somewhat different in these materials due to presence of trapped and defected states in forbidden gap. The significant numbers of charge carriers are present in the forbidden gap, and they don't contribute in field dependent charge propagation, and is considered to be static. The relationship between the applied voltage and current changes according to existence of localized states but behaviour of charge transport doesn't change at initial value of voltage. The understanding of charge transport mechanism occurred with the realization of current, and it can be changed according to conduction through localized states. The charge transport behaviour through these localized states depends upon the density of states and their locality.Figure 4a elucidates the enhancement in dc conductivity as a function of temperature. The dc conductivity of prepared samples increases with the increase in temperature which indicates that prepared samples have semiconducting nature, and the variation in dc conductivity with temperature is almost linear which indicates the strong dependency of charge propagation on temperature as well as on applied electrical field. The electrical conductivity also strongly depends upon Nd_2O_3 doping concentration in ZnO matrix, because dc conductivity increases with the increase in doping concentration as shown in figure 4b.

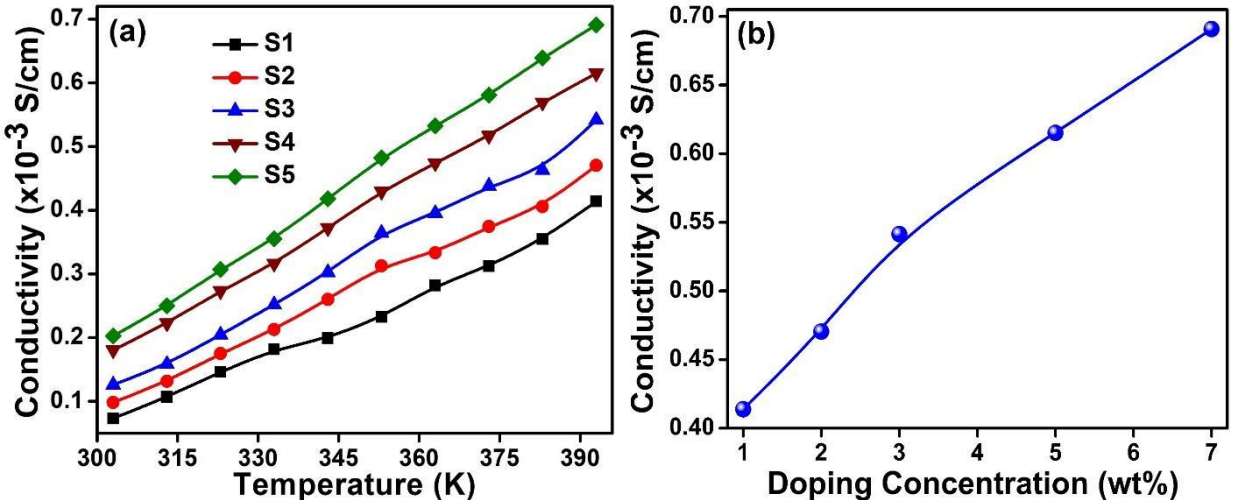

Figure 4: Variation in dc conductivity as function of (a) temperature for S1 (1wt%), S2 (2wt%), S3 (3wt%), S4 (5wt%), S5 (7wt%) composite samples, and (b) doping concentration at temperature 393K.

The localized states may exist with the three possibilities, out of these three possibilities, the first is the presence of localized states between the valence and conduction bands, and this position is known as shallow or deep trap states. The trap states may also exist in lower part of conduction band, and this situation is more likely shallow trap states according to second possibility. Moreover, all conduction states lie in upper side of delocalized states, and the charge carriers of unlocalized states can move freely for the conduction.In these two possibilities, there is enough number of charge carriers/unlocalized states in the conduction band, and conduction is governed by unlocalized states. Now, the third possibility is that complete conduction band is filled with localized states. In this situation, all the charge carriers trapped in localized states in conduction band, and material behave as an insulating material.

Thus in order to find exact mechanism for conduction in present samples, the temperature dependent electrical (dc) conductivity is investigated through various conduction models [22]. The temperature dependence of presently prepared samples can be attributed with the semiconducting behaviour, which can be governed by the expression [23,24]

$$\sigma_{dc} = \sigma_0 exp\left(\frac{-E_A}{k_B T}\right) \qquad (1)$$

Here,σ_0, E_A, K_B, and T are pre-exponential factor, activation energy, Boltzmann constant, and temperature, respectively. It is observed that the variation in dc conduction with temperature is almost linear but not exactly linear. Moreover, the conduction phenomenon is associated with temperature dependent conduction mechanism for which activation energy depends upon temperature. The values of activation energy may are determined by slopes of plots between logarithmic conductivity and 1000/T for all the prepared samples (figure 5a). If these plots are almost linear, then this behaviour has the significant co-relation with the Arrhenius types of charge transport mechanism given by expression (1) which generally occurs in case of band to band conduction. Thus, these samples may be follow Arrhenius model for charge propagation. The calculated values of activation energy using the expression (1) are 0.93, 0.87, 0.83, 0.76, 0.72 meV for samples S1, S2, S3, S4, and S4, respectively.Activation energy decreases with the increase in doping concentration which in turn indicates that electron required lower energy to jump in conduction band from

valence band.Moreover, the temperature dependent charge transport properties of presently prepared samples can also be determined through various types of morphological and structural investigations arising due to conjugation length, oxidation level, types and level of doping, crystallinity, etc.

The charge transport mechanism in prepared composite samples is also investigated using the Kivelson's model because this is also commonly followed model for conduction in various types of materials. According to Kivelson's model, charge carriers move between neutral and charge states [25]. Moreover, according to modified Kivelson's model, the temperature dependent dc conductivity can be estimated by power method [26,27]

$$\sigma_{dc} = AT^{\gamma} \quad (2)$$

$$log\sigma_{dc} = logA + \gamma logT \quad (3)$$

Here, A is constant, and 'γ'is constant power index but have different value for different slopes. If power index 'γ' has value equal to or greater than 10, it shows applicability of Kivelson's model [28]. Therefore, to check the applicability of Kivelson's model, the logarithmic dc conductivity is plotted as function of logarithmic temperature as shown in figure 5b, and fitted with expression (3). The 'γ' is the slope and logA is the intercept of curves, here the calculated values of 'γ' (slope) for S1, S2, S3, S4 and S5 samples are found to be 6.18, 5.77, 5.49, 4.64 and 4.32, respectively. The calculated values of 'γ' are lower than 10 for all the samples which discarded the applicability of Kivelson's model. This further indicates the applicability of Arrhenius model rather the Kivelson's model.

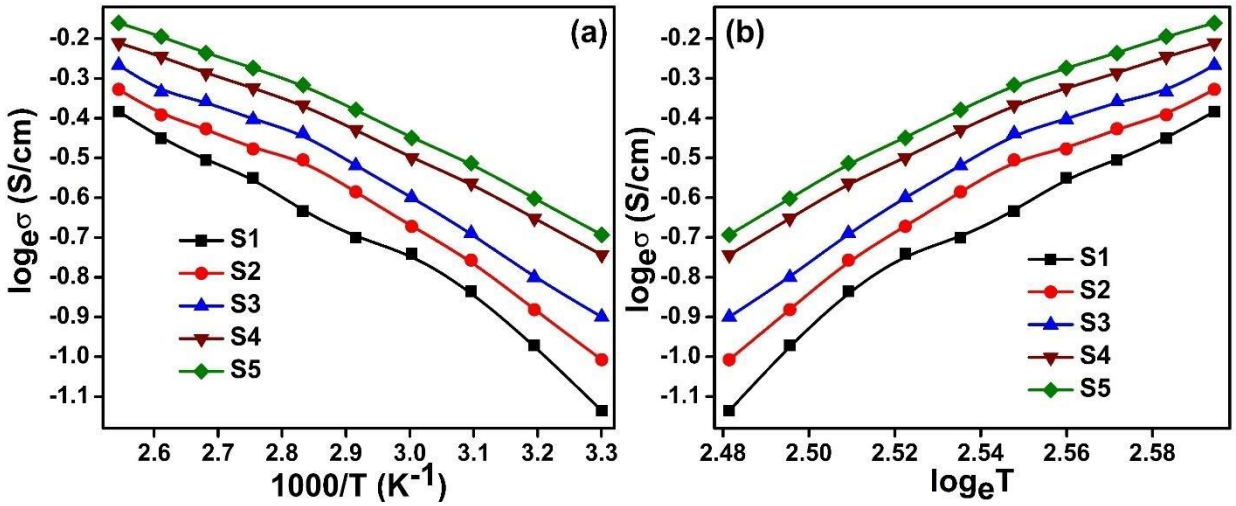

Figure 5: Variation in logarithmic dc conductivity as function of (a) 1000/T, and (b) logarithmic temperature.

Gas sensing Studies

The synthesized samples were subjected to two distinct environment of ethanol (100 and 200ppm) to test their gas sensing behavior. At a fixed applied voltage of 1 V, the electrical current of the prepared samples changes as the environment changes from air to ethanol. Using the relationship below, the percentage response is calculated by comparing the change in electric current of the produced samples with the change in device environment.

$$Response\ (\%) = \frac{\Delta R}{R}\ X\ 100 = \frac{I_g - I_0}{I_o}\ X100 \quad (4)$$

Where I_g and I_o are the current ethanol and ambient air temperatures, respectively. The measuring chamber was emptied to a slightly lower partial pressure value of 500 torr before the ethanol vapors were injected, allowing the ethanol vapors to be easily injected. Before being exposed to ethanol vapors, all of the samples were stabilized to this lower pressure as a baseline for the air environment. When exposed to ethanol vapors, all of the samples' electric current increased with exposure time and ethanol concentrations (100 and 200 ppm), and was saturated in around 100 seconds. The electric current of the samples was observed to diminish when ethanol vapors was removed using a low-capacity rotary pump, and they returned to their nearly-original states after around 100 seconds. With increasing Nd_2O_3 doping concentrations, the electric current of the samples has likewise increased. The increase in electric current in ethanol vapors in prepared composites can be attributed to an increase in charge carrier concentration or increase in charge carrier mobility due to absorption of ethanol vapors in defect states. Figure 6a–e shows the gas sensing responses% derived using Eq. (4) for the all the prepared samples.

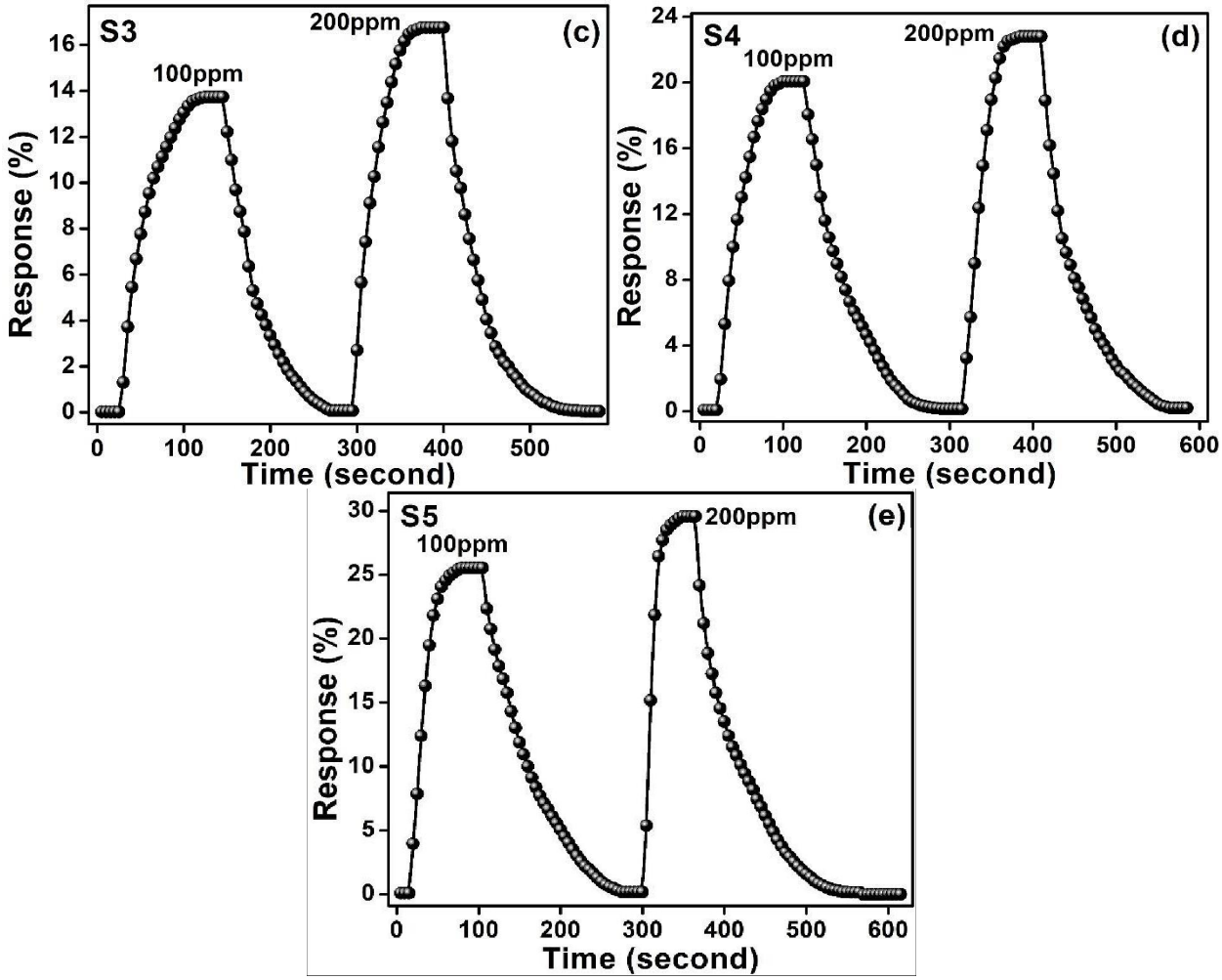

Figure 6: Variation in response (%) as a function of ethanol exposure time and concentration for the samples(a) S1, (b) S2, (c) S3, (d) S4 and (e) S5.

The response values for the prepared composite samples increase as the ethanol vapors concentration (100 to200 ppm) and Nd_2O_3 doping concentration are increased. When the ethanol concentration is increased, the response of the pristine sample (PANI)

increases. Furthermore, raising the doping concentration from 1 to 7 wt%t at 200 ppm of ethanol vapors enhances the responsiveness of the produced samples from 9.86 to 29.57%.Another important parameters of vapors detection measurements such as response and recovery time were investigated using the obtained data. From these data, it is observed that the response time of prepared devices decreases with the increase in doping concentration whereas recovery time was decreases.

Conclusion

Using the thermal evaporation technique, ZnO/Nd_2O_3 nanocomposites were deposited on glass substrates, and the structural, vibrational spectroscopy, morphological properties were systemically investigated. XRD pattern contains some intense peaks with broad hump which indicates prepared samples have semi-crystalline nature. FESEM image of S5 sample indicates that the prepared sample have nanowire morphology having diameter 15-20 nm and length 100 nm. The existence of all required fundamental bands in FTIR spectrum, and investigation from XRD and FESEM suggest the growth of desired samples. The prepared samples may follow Arrhenius's model for charge transport mechanism because the relative curve between logarithmic dc conductivity and 1000/T is almost linear. That means charge propagation will be as band to band conduction for presently prepared samples, and due to lower value of power index than 10 in Kivelson's model, the Kivelson's model is discarded out.The ethanol vapors detection measurements of prepared samples were investigated at 100 and 200 ppm levels and it is observed that the response% increases with the increase in doping level as well as increase in ethanol vapors environment.

References

[1] Reda M. Mohamed, Adel. A. Ismail, Mohammad W. Kadi, Ajayb S. Alresheedi, Ibraheem. A. Mkhalid,Photocatalytic performance mesoporous Nd2O3 modified ZnO nanoparticles with enhanced degradation of tetracycline,Catalysis Today,Volume 380,2021, Pages 259-267. https://doi.org/10.1016/j.cattod.2020.11.002.

[2] D. Durgalakshmi, S. Prabha, J. Mohanraj, R. Ajay Rakkesh, R. Saravanan,Hybrid ZnO nanostructures modified graphite electrode as an efficient urea sensor for environmental pollution monitoring,Chemosphere,2022,133918,https://doi.org/10.1016/j.chemosphere.2022.133918.

[3] Fangda Ren, Chaonan An, Yongde Yan, Valeri Smolenski, Alena Novoselova, Yun Xue, Fuqiu Ma, Milin Zhang,Synthesis of ZIT composite material and immobilization of Nd2O3,Ceramics International,2022,https://doi.org/10.1016/j.ceramint.2022.02.088.

[4] Richa Mishra, M. Goswami, A.K. Arya,Studies on phase evolution, microstructure and crystallization kinetics in Nd2O3 doped Li2O-Al2O3-SiO2 glass system,Journal of Non-Crystalline Solids,Volume 582,2022, 121441. https://doi.org/10.1016/j.jnoncrysol.2022.121441.

[5] M.G. Nair, M. Nirmala, K. Rekha, A. Anukaliani, Structural, optical, photo catalyticand antibacterial activity of ZnO and Co doped ZnO nanoparticles, Mater. Lett. 65(2011) 1797–1800, https://doi.org/10.1016/j.matlet.2011.03.079.

[6] Zarnish Sabir, Mehwish Akhtar, Sonia Zulfiqar, Shagufta Zafar, Philips O. Agboola, Sajjad Haider, Sameh A. Ragab, Muhammad Farooq Warsi, Imran Shakir,L-Cysteine functionalized Nd2O3/rGO modified glassy carbon electrode: A new sensing strategy for the rapid, sensitive and simultaneous detection of toxic nitrophenol isomers,Synthetic Metals,Volume 277,2021, 116774. https://doi.org/10.1016/j.synthmet.2021.116774.

[7] Chaoyu Lin, Qingyang Li, Huanzhu Guang, Maozhong An,Electrodeposited Zn: A promising alternative to ZnO seed layer for hydrothermal growth of ZnO nanowire array,Materials Letters,Volume 314,2022,131848,https://doi.org/10.1016/j.matlet.2022.131848.

[8] M. Gusatti, D.A.R. Souza, N.C. Kuhnen, H.G. Riella, Growth of variable aspect ratioZnO nanorods by solochemical processing, J. Mater. Sci. Technol. 31 (2015) 10–15,https://doi.org/10.1016/j.jmst.2014.08.001.

[9] M. Gusatti, C.E.M. Campos, D.A.R. Souza, N.C. Kuhnen, H.G. Riella, P.S. Pizani,Effects of reaction temperature on structural properties of ZnO nanocrystals preparedvia solochemical technique, J. Nanosci. Nanotechnol. 12 (2012) 7986–7992,https://doi.org/10.1166/jnn.2012.6646.

[10] Dongwan Kim, Jae-Young Leem,Synthesis of interface modified MoS2/ZnO heterostructure via simple hydrothermal method and their enhanced UV photodetection characteristics with ultrafast photoresponse speed,Materials Research Bulletin,Volume 150,2022,111767,ISSN 0025-5408,https://doi.org/10.1016/j.materresbull.2022.111767.

[11] C. Chen, B. Yu, P. Liu, J. Liu, L. Wang, Investigation of nano-sized ZnO particlesfabricated by various synthesis routes, J. Ceram. Process. Res. 12 (2011) 420–425.

[12] Abdul Raouf Malik, Sadia Sharif, Fozia Shaheen, Mansoor Khalid, Yasir Iqbal, Abrar Faisal, Muhammad Hammad Aziz, Muhammad Atif, Shafiq Ahmad, M. Fakhar-e-Alam, Nazia Hossain, Hijaz Ahmad, Thongchai Botmart,Green synthesis of RGO-ZnO mediated Ocimum basilicum leaves extract nanocomposite for antioxidant, antibacterial, antidiabetic and photocatalytic activity,Journal of Saudi Chemical Society,Volume 26, Issue 2,2022,101438.
https://doi.org/10.1016/j.jscs.2022.101438.

[13] Dongwan Kim, Jae-Young Leem,Modified interfaces of ZnO thin films through MoS2 addition in precursor solution for MoS2/ZnO heterojunctions and their enhanced ultraviolet photodetection properties,Journal of Alloys and Compounds,Volume 905,2022, 164168. https://doi.org/10.1016/j.jallcom.2022.164168.

[14] K. Bouras, G. Schmerber, D. Aureau, H. Rinnert, G. Ferblantier, T. Fix, S. Colis,P. Bazylewski, B. Leedahl, A. Etcheberry, G.S. Chang, A. Dinia, A. Slaoui, Insightinto photon conversion of Nd3+ doped low temperature grown p and n type tinoxide thin films, RSC Adv. 6 (2016) 67157–67165, https://doi.org/10.1039/C6RA14460H.

[15] B. Shahmoradi, K. Soga, S. Ananda, R. Somashekar, K. Byrappa, Modification ofneodymium-doped ZnO hybrid nanoparticles under mild hydrothermal conditions,Nanoscale 2 (2010) 1160, https://doi.org/10.1039/c0nr00069h.

[16] A.S.H. Hameed, C. Karthikeyan, A.P. Ahamed, N. Thajuddin, N.S. Alharbi,S.A. Alharbi, G. Ravi, In vitro antibacterial activity of ZnO and Nd doped ZnOnanoparticles against ESBL producing Escherichia coli and Klebsiella pneumoniae,Sci. Rep. 6 (2016) 1–11, https://doi.org/10.1038/srep24312.

[17] Anindita Samanta, M.N. Goswami, P.K. Mahapatra, Influence of Nd3+ doping inZnO nanoparticles to enhance the optical and photocatalytic activity, Mater. Res.Express 6 (2019), https://doi.org/10.1088/2053-1591/ab0c25.

[18] S. Vijayakumar, A.K. Ponnalagi, S. Nagamuthu, G. Muralidharan, Microwave assistedsynthesis of Co3O4 nanoparticles for high-performance supercapacitors,Electrochim. Acta 106 (2013) 500–505.

[19] Nuno P.F. Gonçalves, Mirtha A.O. Lourenço, Simone R. Baleuri, Stefano Bianco, Pravin Jagdale, Paola Calza,Biochar waste-based ZnO materials as highly efficient photocatalysts for water treatment,Journal of Environmental Chemical Engineering,Volume 10, Issue 2,2022, 107256.
https://doi.org/10.1016/j.jece.2022.107256.

[20] G. Dhamale, V. Mathe, S. Bhoraskar, S. Sahasrabudhe, S. Dhole, S. Ghorui, Synthesisand characterization of Nd2O3 nanoparticles in a radiofrequency thermal plasmareactor, Nanotechnology 27 (2016) 085603.

[21] A. Anžlovar, Z.C. Orel, K. Kogej, M. Žigon, Polyol-mediated synthesis of zinc oxidenanorods and nanocomposites with poly (methyl methacrylate), J. Nanomater.2012 (2012) 31.

22 M. Sharma, D. Singh, A. Menon, G. Madras, S. Bose,Suppressing Electromagnetic Radiation by Trapping Ferrite Nanoparticles and Carbon Nanotubes in Hierarchical Nanoporous Structures Designed by Crystallization-Induced Phase Separation, *Chem. Sel.***2018**, *3*, 1189–1201.

23 K. Manna, S. K. Srivastava, V. Mittal, Role of Enhanced Hydrogen Bonding of Selectively Reduced Graphite Oxide in Fabrication of Poly(vinyl alcohol) Nanocomposites in Water as EMI Shielding Material, *J. Phys. Chem. C.***2016**, *120*, 17011−17023.

24 L. Ma, Z. Lu, J. Tan, J. Liu, X. Ding, N. Black, T. Li, J. Gallop, L. Hao, Transparent Conducting Graphene Hybrid Films To Improve Electromagnetic Interference (EMI) Shielding Performance of Graphene, *ACS Appl. Mater. Interfaces.***2017**, *9*, 34221−34229.

25 V. Bhingardive, T. Woldu, S. Biswas, G. P. Kar, S. Thomas, N. Kalarikkal, S. Bose,Microwave Absorption in MWNTs-Based Soft Composites Containing Nanocrystalline Particles as Magnetic Core and Intrinsically Conducting Polymer as a Conductive Layer, *Chem. Sel.***2016**, *1*, 4747 – 4752.

26 S. Kim, J. S. Oh, M. G. Kim, W. Jang, M. Wang, Y. Kim, H. W. Seo, Y. C. Kim, J. H. Lee, Y. Lee, J. D. Nam, Electromagnetic Interference (EMI) Transparent Shielding of Reduced Graphene Oxide (RGO) Interleaved Structure Fabricated by Electrophoretic Deposition,*ACS Appl. Mater. Interfaces.***2014**, *6*, 17647−17653.

27 I. Rawal, O. S. Panwar, R. K. Tripathi, A. P. Singh, S. K. Dhawan, A. K. Srivastava, Effect of helium gas pressure on dc conduction mechanism and EMI shielding properties of nanocrystalline carbon thin films, *Mater. Chem. Phys.* **2015,***158*, 10-17.

28 P. K. Choudhury, S. Ramaprabhu, K. P. Ramesh, R. Menon, Correlated conformation and charge transport in multiwall carbon nanotube-conducting polymer nanocomposites, *J. Phys.: Condens. Matter.***2011**, *23*, 265303-1-8.